Nenad Kranjčević
Milenko Stegić
Mario Vukšić

ISSN 1333-1124

LOADING OF PIPELINE SUPPORTS IN A MICRO-TUNNEL

UDC 621.644:624.19:516.6

Summary

Micro-tunnelling is a trenchless method for the application of underground utilities. If a tunnel is built as a shallow arc beneath obstacles, the insertion of steel pipeline presents a particular difficulty. A computational model has been developed in order to investigate the loading of pipeline wheel supports and the stresses in pipes during the insertion. The model is based on beam elements and includes the unilateral contact problem, which is solved by the iteration procedure presented in the paper. The results of simulations for four different paths are discussed and the improved path of the micro-tunnel is proposed.

Key words: *micro-tunnel, steel pipeline, insertion process, support load, beam elements*

1. Introduction

Trenchless construction methods, including horizontal directional drilling (HDD) and micro-tunnelling, are nowadays widely used to construct utilities within busy urban areas, underground waterways, or other natural or manmade barriers. HDD refers to a steerable system for the installation of pipes, conduits and cables in a shallow arc using a drill rig at the ground surface. The main problems of HDD modelling are dealt with in [1,2] while the pulling process of the pipes and other facilities in direct contact with the soil is discussed in detail in [3,4]. Micro-tunnelling is a procedure that uses a remotely-controlled, small diameter tunnel boring machine [5]. Sometimes the path of a micro-tunnel is made as a direct line between two vertical shafts at jacking locations, but sometimes, similarly to the HDD, a micro-tunnel is built as a shallow arc beneath the obstacles. The problem of pipes laid down at the bottom of the tunnel is similar to the problem of placing a pipe on an uneven surface [6,7], but, with a discrete setup of supports, it can be more closely connected to the problems discussed in [8-10].

1.1 Micro-tunnel

A micro-tunnel made of concrete pipes, first of its kind in Croatia, was set under the Sava River. It is approximately 1 km long, with the lowest point 18 m below the entrance. Its inner diameter is 1.6 m. The accurate line of the tunnel was known from the geodetic recordings. The line of the tunnel consisted of two straight sections: the entering section descending at an angle of 2.5° and the exiting section ascending at an angle of 2°. The third section of the tunnel between those two was a curved section with a radius of curvature of approximately 1 km (Fig.1).

A package of pipes was to be inserted into the tunnel. The package contained two steel pipes of nominal diameters of 0.5 and 0.7 m for gas and a PE pipe of a smaller diameter (approx. 0.2 m) for optical fibres. In the further analysis, the PE pipe is neglected.

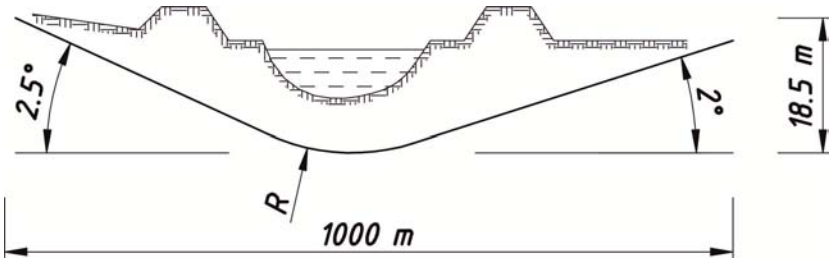

Fig. 1 Longitudinal line of the micro-tunnel

The pipes were inserted in sections. Each pipe section, 150 meters long, consisted of smaller parts welded together and laid down on the ramp in front of the tunnel. Welded pipes were first sealed at both ends and then it was verified that they were leak proof. They were joined to form a package on wheel supports suitable for insertion. The pipes were pulled into the tunnel with a steel cable drawn by a tracked vehicle from the other side of the tunnel. In the next step, a new section was laid down in front of the tunnel and attached to the end of the pipeline drawn in. The procedure was repeated until the whole pipeline was placed in the micro-tunnel. During the insertion process the water from the tunnel was pumped out. In the final stage, the tunnel, together with the pipes, was flooded. The first section of the pipeline in front of the tunnel is shown in Figure 2.

Fig. 2 Package of pipes in front of the tunnel

Fig. 3 Bent structure of the support

1.2 Insertion problems

The first attempt to insert a pipe section failed in spite of the great number of light structural supports and their arrangement (Fig. 3). A high degree of stiffness of steel pipes was the main reason why the attempt with the disposition of supports at short distances failed. The load was not equally distributed to the supports because of the difference between the elastic line of the pipes and the line (path) of the tunnel.

2. New supports with increased load capacity

Due to the problems encountered with original supports, stronger supports with lager wheels and 150 kN load capacity were designed. New supports (Fig. 4) were designed with one main wheel guided on a steel angle fixed at the bottom of the tunnel and two auxiliary wheels in the upper zone, directly in contact with the concrete wall of the tunnel. The purpose

of the auxiliary wheels was to take over the side force and to guide the supports in the case when the lifting of the supports fills the clearance.

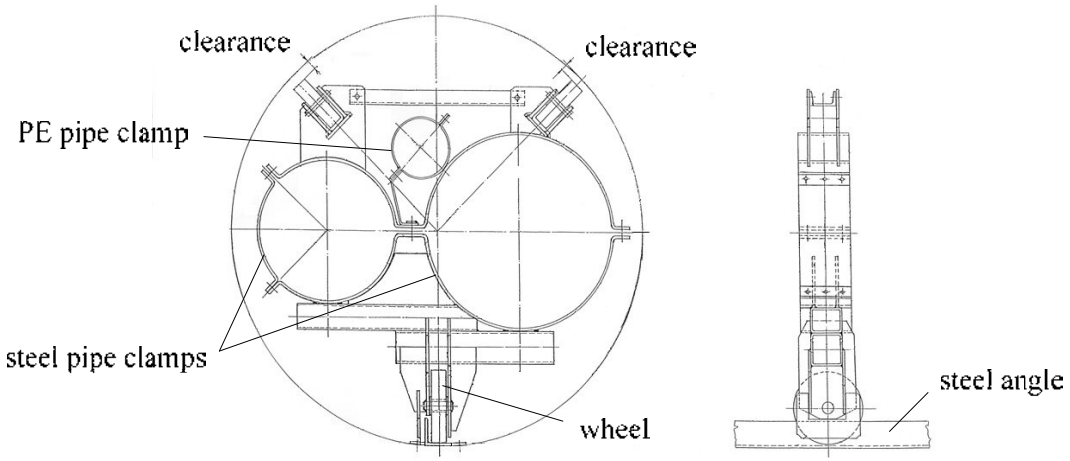

Fig. 4 Improved design of the wheel support with clamps. Single main wheel rolling on the steel angle rail and two side wheels designed to establish direct contact with the walls of the tunnel.

3. Formulation of the problem

The main issue was to determine the position of supports in the process of inserting the pipes into the tunnel in order to meet the following conditions: not to exceed the maximum allowable force exerted on a single support, to avoid contacts with the ceiling of the tunnel, and to satisfy the strength requirements for both pipes. Thus, for a given position of the supports, the problem during the insertion process was to find the following:

- maximal load on supports,
- maximal lifting of supports, and
- maximal bending moments, i.e. maximal stresses in both steel pipes.

4. Numerical solution

Numerical solution is achieved by employing beam elements and iteration procedure encoded in the MATLAB package.

4.1 Mechanical model

It is assumed that the main load of the pipe package is its own weight, while the weight of the supports and the pulling force or any axial load of the pipes are neglected. It is also assumed that the supports and the micro-tunnel are of negligible compliance.

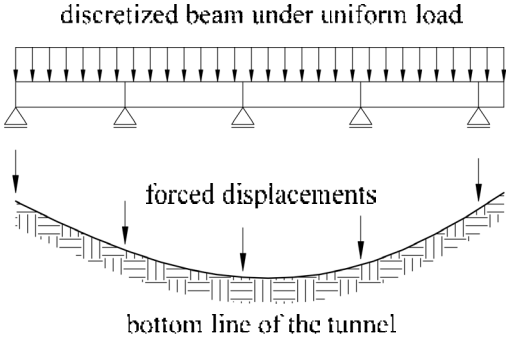

Fig. 5 Mechanical model - general approach

Each pipe is divided into $(n-1)$ beam elements with known (forced) displacements of support joints (see Fig. 5). Two pipes are connected together with the clamps of wheel supports. This is taken into account in the mechanical model by coupling the vertical displacements of these joints (Fig. 6).

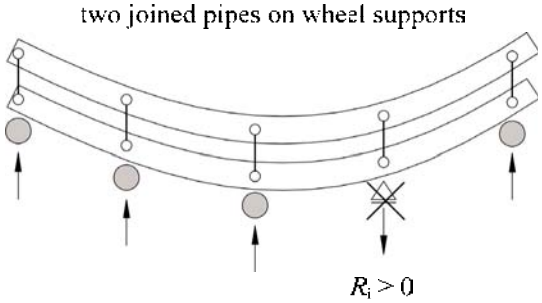

Fig. 6 Mechanical model of two joined pipes

Forced support displacements can give positive reactions of some supports for a given position of the pipes in the tunnel. Considering that this condition is not realistic, these supports have to be set as inactive and the new configuration has to be calculated. Unfortunately, it is still possible that some of the inactivated supports are, in the next step, sagged to take the load. Because of that, the iteration procedure presented in subsection 4.3 enables the pipe-package to be settled down in a proper configuration, i.e. to retain only the unloaded supports released from the bottom of the tunnel.

4.2 Beam element

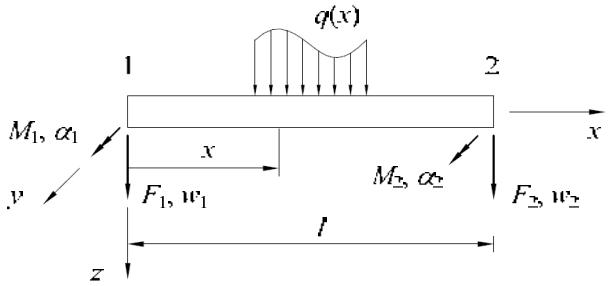

Fig. 7 Beam element

Stiffness matrix of beam element *e* according to [11] is

$$\mathbf{K}_e = \begin{bmatrix} {}^e\boldsymbol{\kappa}_{11} & {}^e\boldsymbol{\kappa}_{12} \\ {}^e\boldsymbol{\kappa}_{21} & {}^e\boldsymbol{\kappa}_{22} \end{bmatrix} \tag{1}$$

where

$${}^e\boldsymbol{\kappa}_{11} = \frac{EI_y}{l^3}\begin{bmatrix} 12 & -6l \\ -6l & 4l^2 \end{bmatrix}, \quad {}^e\boldsymbol{\kappa}_{12} = \frac{EI_y}{l^3}\begin{bmatrix} 12 & -6l \\ 6l & 2l^2 \end{bmatrix},$$

$${}^e\boldsymbol{\kappa}_{21} = \frac{EI_y}{l^3}\begin{bmatrix} -12 & 6l \\ -6l & 2l^2 \end{bmatrix} \quad \text{and} \quad {}^e\boldsymbol{\kappa}_{22} = \frac{EI_y}{l^3}\begin{bmatrix} 12 & 6l \\ 6l & 4l^2 \end{bmatrix}. \tag{2}$$

Generalized force vector is given as

$$\mathbf{f}_e = \begin{bmatrix} {}^e\mathbf{g}_1 \\ {}^e\mathbf{g}_2 \end{bmatrix} \tag{3}$$

where ${}^e\mathbf{g}_1 = \begin{bmatrix} F_1 \\ M_1 \end{bmatrix} = q\begin{bmatrix} l/2 \\ -l^2/12 \end{bmatrix}$ and ${}^e\mathbf{g}_2 = \begin{bmatrix} F_2 \\ M_2 \end{bmatrix} = q\begin{bmatrix} l/2 \\ l^2/12 \end{bmatrix}$ for the uniformly distributed weight $q(x)$. For a chained structure of beam elements with $(n-1)$ elements and n nodes, the stiffness matrix of pipe p $(p=1,2)$ becomes the three diagonal matrix,

$$\mathbf{K}_p = \begin{bmatrix} {}^1\boldsymbol{\kappa}_{11} & {}^1\boldsymbol{\kappa}_{12} & \mathbf{0} & \cdots & \mathbf{0} \\ {}^1\boldsymbol{\kappa}_{21} & {}^1\boldsymbol{\kappa}_{22} + {}^2\boldsymbol{\kappa}_{11} & {}^2\boldsymbol{\kappa}_{12} & \cdots & \mathbf{0} \\ \mathbf{0} & {}^2\boldsymbol{\kappa}_{21} & {}^2\boldsymbol{\kappa}_{22} + {}^3\boldsymbol{\kappa}_{11} & \cdots & \mathbf{0} \\ \vdots & \vdots & \vdots & \ddots & {}^n\boldsymbol{\kappa}_{12} \\ \mathbf{0} & \mathbf{0} & \mathbf{0} & {}^n\boldsymbol{\kappa}_{21} & {}^n\boldsymbol{\kappa}_{22} \end{bmatrix} \tag{4}$$

the generalized force vector,

$$\mathbf{f}_p = \left[{}^1\mathbf{g}_1^{\mathrm{T}}, {}^1\mathbf{g}_2^{\mathrm{T}} + {}^2\mathbf{g}_1^{\mathrm{T}}, {}^2\mathbf{g}_2^{\mathrm{T}} + {}^3\mathbf{g}_1^{\mathrm{T}}, \ldots, {}^n\mathbf{g}_2^{\mathrm{T}} \right]^{\mathrm{T}} \tag{5}$$

and the generalized displacement vector

$$\mathbf{x}_p = \left[w_1, \alpha_1, w_2, \alpha_2, \ldots, w_n, \alpha_n \right]^{\mathrm{T}} \tag{6}$$

of one pipe, where w_i and α_i $(i=1,2,...,n)$ are the node lateral displacements and angular displacements, respectively.

If the stiffness matrix of the first pipe is denoted as $\mathbf{K}_1$ and of the second pipe as $\mathbf{K}_2$, force vectors as $\mathbf{f}_1$ and $\mathbf{f}_2$, and the generalized displacement vectors as $\mathbf{x}_1$ and $\mathbf{x}_2$, respectively, then the linear equation of two-pipe package can be written as

$$\mathbf{K}\mathbf{x} = \mathbf{E}\mathbf{f} \tag{7}$$

where $\mathbf{K} = \begin{bmatrix} \mathbf{K}_1 & \mathbf{0} \\ \mathbf{0} & \mathbf{K}_2 \end{bmatrix}$, $\mathbf{f} = \begin{bmatrix} \mathbf{f}_1 \\ \mathbf{f}_2 \end{bmatrix}$, $\mathbf{x} = \begin{bmatrix} \mathbf{x}_1 \\ \mathbf{x}_2 \end{bmatrix}$ and $\mathbf{E}$ is the identity matrix of order $4n$.

4.3 Boundary conditions

In the place of each support it is assumed that the clamp allows different angular joint displacements, but in the lateral direction they must be tied together. If the support is inactive, i.e. lifted from the bottom of the tunnel, displacements of adjoining nodes are unknown, but must be considered equal. This is achieved by setting the translational stiffness and the loads of corresponding two adjoined displacements to the first one, while the second displacement is decoupled from all other coordinates. Thus, the system maintains its order and all of its variables.

For example, if i and j $(j = i + 2n)$ are indices of inactive adjoined coordinates in the global vector ***x***, then the *j*-th column of the stiffness matrix **K** has to be added to the *i*-th column and the *j*-th row of both the stiffness matrix **K** and the force vector **f** have to be added

to the *i*-th row. All elements of the *j*-th row of **K** and **f** and the *j*-th column of **K** must then be set to zero except $K(j,i)=-1$ and $K(j,j)=1$, which indicates the condition $w_i - w_j = 0$.

In this way the program calculates active support reactions acting on both pipes.

4.4 Linear equation of the system

There are mixed known and unknown forces and displacements on both sides of equation (7). Because of that, equation (7) is rearranged to the form

$$\mathbf{A}\mathbf{y} = \mathbf{D}\mathbf{b} \tag{8}$$

by interchanging the columns corresponding to the active supports between matrices **K** and **E**, and by changing the sign of these columns. Thus, **K** and **E** become **A** and **D**, respectively. Force vector **f**, with forced displacements on active coordinates, becomes **b**, while the vector **y** contains all unknowns of the system: unknown forces of active supports and unknown displacements of all other coordinates.

4.5 Iteration procedure

Supports with nonnegative reactions must be excluded from the set of active supports for they are just passively hanging on the pipes.

```
ACTIVE=SUPPORTS; % SUPPORTS is vector of support indices
INACTIVE=[];
EXCLUDE=[];
INCLUDE=[];

[REACTIONS,DISPLACEMENTS]=f(ACTIVE,INACTIVE,FORCED_DISPLACEMENTS);

EXCLUDE=find(REACTIONS>=0);

while ((~isempty(EXCLUDE))|(~isempty(INCLUDE)))

    INACTIVE=[INACTIVE;ACTIVE(EXCLUDE)];
    ACTIVE(EXCLUDE)=[];

   [REACTIONS,DISPLACEMENTS]=f(ACTIVE,INACTIVE,FORCED_DISPLACEMENTS);

    INCLUDE=find((FORCED_DISPLACEMENTS < DISPLACEMENTS(SUPPORTS)));

    if ~isempty(INCLUDE)
        for i=INCLUDE
            ACTIVE=sort([ACTIVE;SUPPORTS(i)]);
            INDEX=find(INACTIVE==SUPPORTS(i));
            INACTIVE(INDEX)=[];
        end

       [REACTIONS,DISPLACEMENTS]=f(ACTIVE,INACTIVE, FORCED_DISPLACEMENTS);
    end

    EXCLUDE=find(REACTIONS>=0)
end
```

Fig. 8 Simplified MATLAB code of iteration procedure for support lifting control

One way of dealing with the problem of the unilateral contacts is to start from support contact conditions

$$\left(\text{if } w_i < w_{ti} \text{ then } R_i = 0 \text{ and if } w_i = w_{ti} \text{ then } R_i < 0\right) \tag{9}$$

where w_i are the support displacements, w_{ti} the tunnel coordinates and R_i the reaction of i-th support. Equation (9) can be further solved [8] by minimizing the potential energy of the discretized pipes, which leads to the inequality constrained quadratic optimization problem. Instead of that, in this paper, a simple iteration procedure was used.

Figure 8 shows the algorithm of iteration procedure for settling down the pipes for a given inserting position. Function f(ACTIVE, INACTIVE, FORCED_DISPLACEMENTS) takes into account, among other variables, active supports and, as a result, gives reactions on these supports as well as displacements at the places of inactive ones. For each step, the results are recorded and presented in animated form in 1 m steps of the insertion process (Figs 10, 12, 14, 16).

Once the lifting tends to exceed the clearance in the tunnel (Fig. 4), the supports are allowed to push against the upper side of the tunnel. The presented procedure can be improved by taking into account the clearance, but in this study a simpler version of the procedure was used because the upper contact never occurred in simulations.

5. Results of simulations

In this section, the results of four different simulated cases are presented and discussed. Each case involves a different curve, but all of them are made by cubic spline interpolation through discrete points, as in the following case:

1. The first path of the built tunnel is given by recorded coordinates of discrete points, while the full curve is replaced by cubic spline interpolation (Fig. 9a).

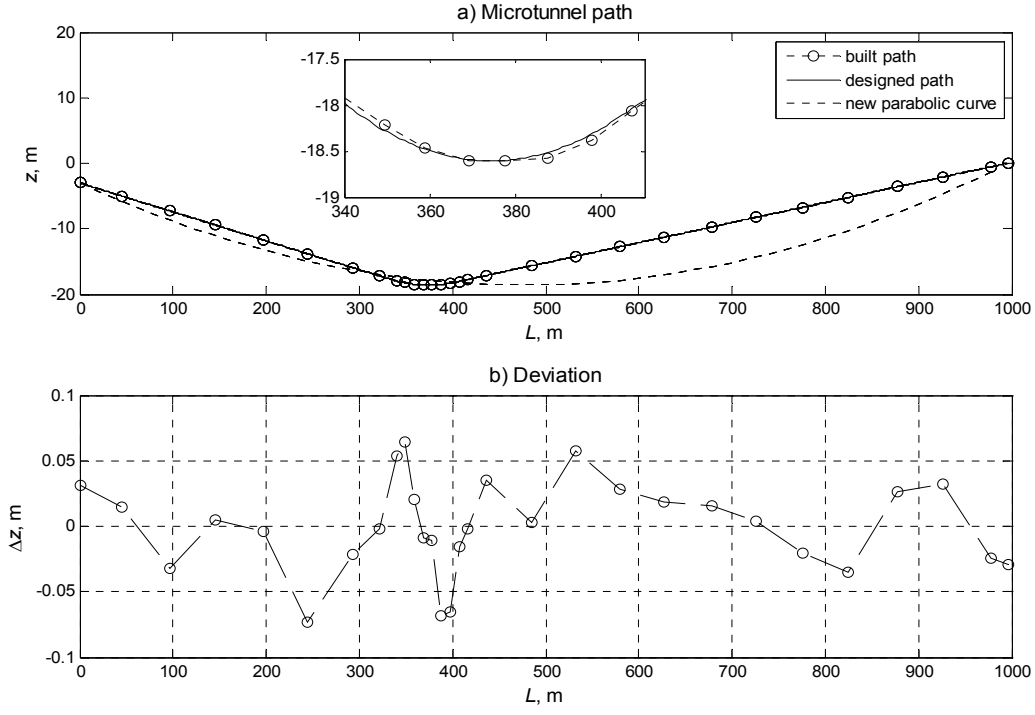

Fig. 9 Simulated micro-tunnel cases: a) different micro-tunnel paths and b) deviations of the built path from the designed path

2. The second path is a combination of two linear segments connected with an arc of constant curvature, as it was designed. Deviations of the designed path from the recorded coordinates are minimized by the least square method. These deviations are shown in Figure 9b. The tolerances of deviations of a tunnel path on line and level are generally specified in the order of ± 50 mm and ± 75 mm, respectively [12].
3. The third path is a parabolic curve connecting the end points of the micro-tunnel [13] and it has the same depth as the previous paths.
4. The fourth path is made from the ideal parabolic curve 3 by adding deviations of the built path 1 from the designed path 2. The path achieved in this way is more realistic than the ideal parabola.

MATLAB routines are written to give an animated output of the pipe-package of constant length in different pulling-in positions in the tunnel. Figure 10a shows the global position, while Figure 10b gives a critical tunnel section zoomed in. R_1 and R_1 are two maximal support reactions of the shown step. Lifted supports are presented as hollow circles, while active supports are circles filled with stars. Displacements of the pipe of greater diameter are given in Figure 10c and can be used for the control of support lifting. Figure 10d shows bending moment diagrams and maximal stresses of both pipes.

The maximal stress values are directly correlated with bending moments by a well-known equation

$$\sigma_{\mathrm{f\,max}} = M_{\mathrm{f\,max}} / W_y \tag{10}$$

where $\sigma_{\mathrm{f\,max}}$ is the maximal normal stress in the pipe, $M_{\mathrm{f\,max}}$ the maximal bending moment, and W_y the elastic section modulus of pipe cross section.

Figures 10, 12, 14, and 16 present outputs of final simulated positions of four different micro-tunnel paths. In each simulation the total length of pipes is 306 m. There are 39 supports placed at 8 meter distance and 2 m overhang on the right side. Pipes are “pulled” to the right.

A computational model is developed to determine the optimal distance between supports in the micro-tunnel in order to reduce the support loading. The critical point in the tunnel is considered to be the transition from the descending to the ascending line. In this section of the tunnel, the elastic line of steel pipes does not follow the path of the tunnel and the widest span between two active supports is 32 meters (Fig. 10b, c). Nevertheless, the maximal support reactions are less than the allowable support load of 150 kN. Stress requirements are also achieved for both pipes. Figure 11 shows reactions of six leading supports in every insertion step.

Several assumptions have been made when developing this computational model. In particular, the compliance of the tunnel is considered negligible. However, in reality, it is not completely negligible and, as a result, inactive supports may become active and partially loaded. The final choice of distances between supports is made on the basis of the allowable amount of ready-made supports and the aforementioned analysis.

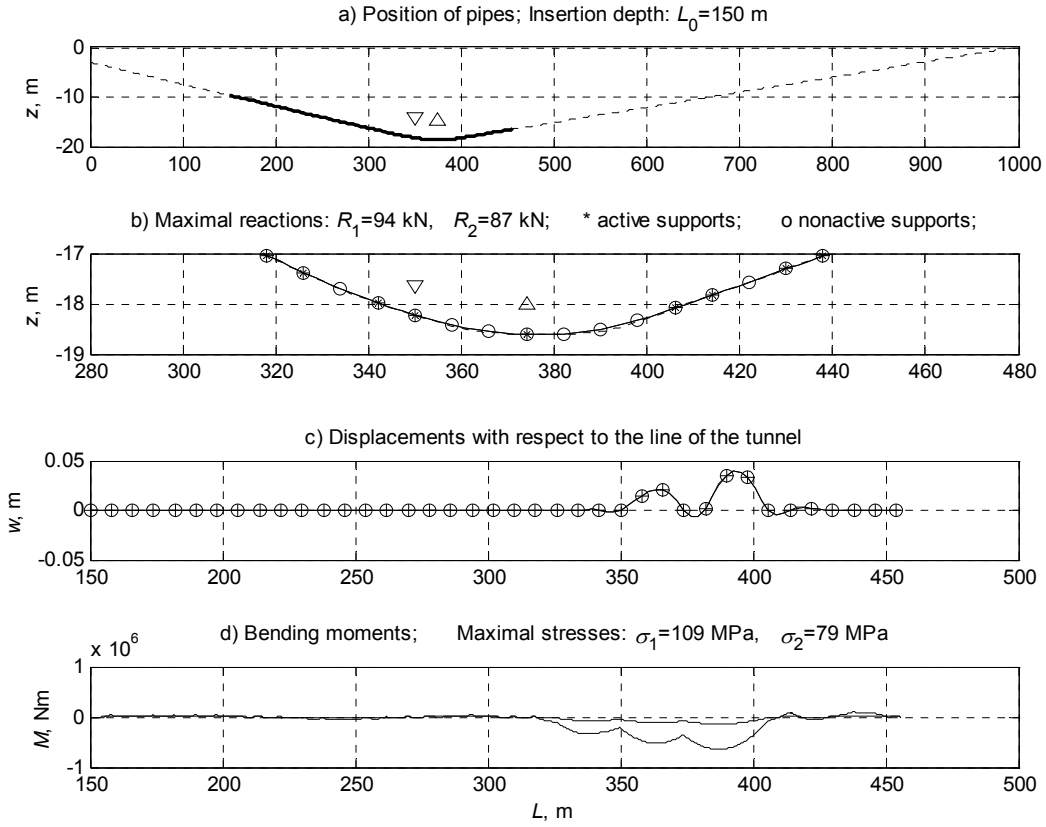

Fig. 10 Simulated insertion process at a given position of the pipe package segment in the micro-tunnel: a) position of the pipe package section, b) two maximal support reactions zoomed in and labelled, c) displacements of bigger diameter pipe and d) bending moments and maximal stresses of both pipes

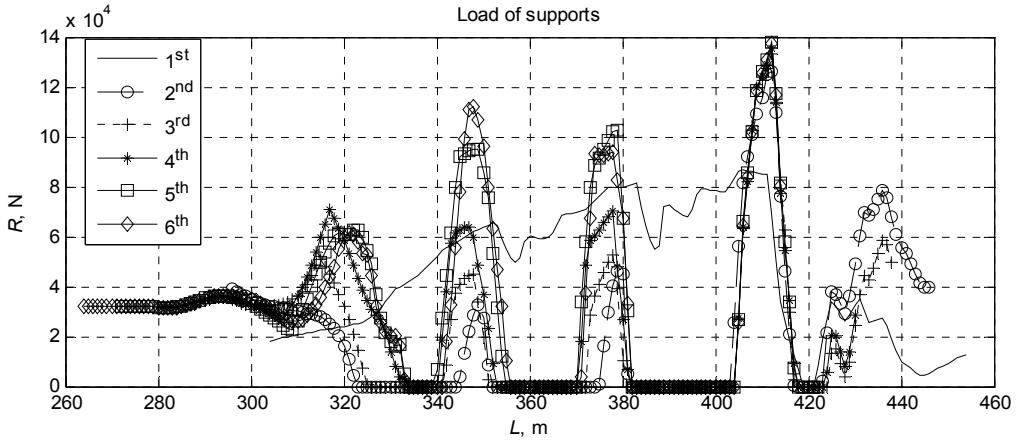

Fig. 11 Reactions of six leading supports during simulated insertion; the path of the micro-tunnel as it was built

Furthermore, additional simulations were carried out to find out how much the path influences support loads and pipe stresses. If the tunnel was constructed perfectly, as it was designed, with linear descending and ascending sections and an arc of a constant radius between them, the support reactions and pipe stresses would be reduced by up to 20 % (Fig. 12 and 13).

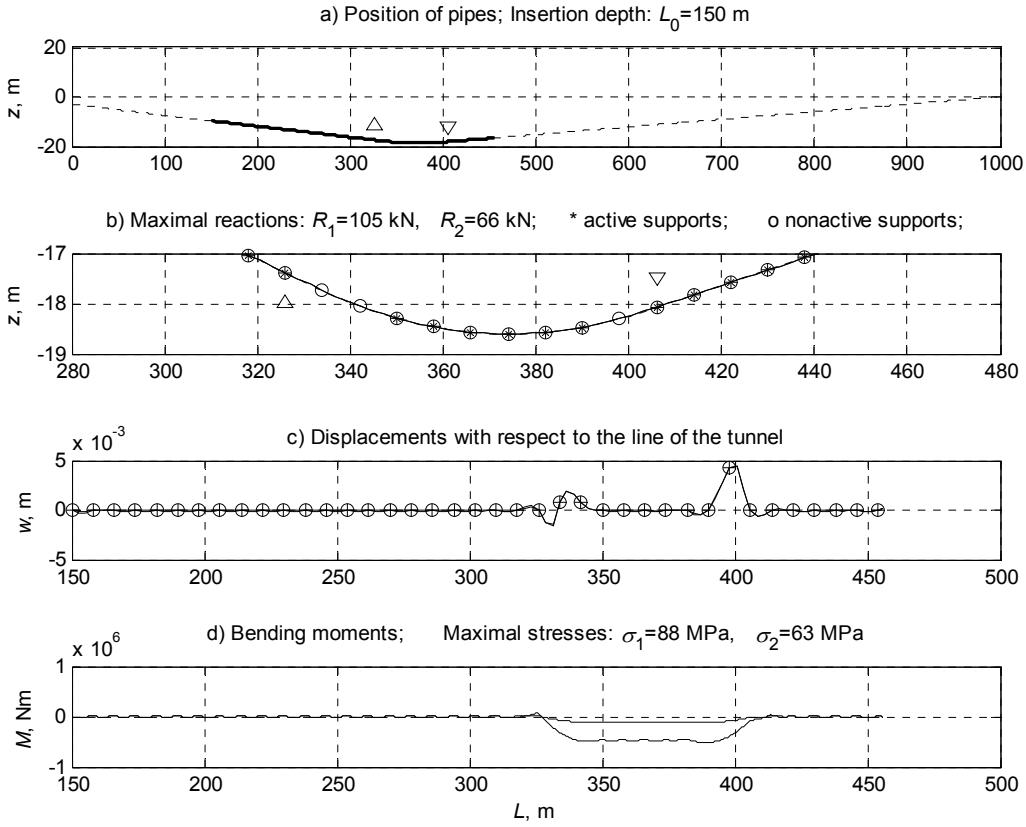

Fig. 12 Simulated insertion process at a given position of the pipe package segment in the micro-tunnel; the tunnel path is considered to be a designed curve consisting of three ideal parts: linear descending part, circular arc, and linear ascending part

The nature of the path curve with common tangents in connection points still shows sudden changes in second derivatives. The radius of curvature at the connection point between the linear and the circular path drops from infinity to a constant value, while the second derivative of the elastic line of the pipe remains smooth. In Figure 12c one can notice that the supports in the vicinity of connection points are lifted because of the previously mentioned reason.

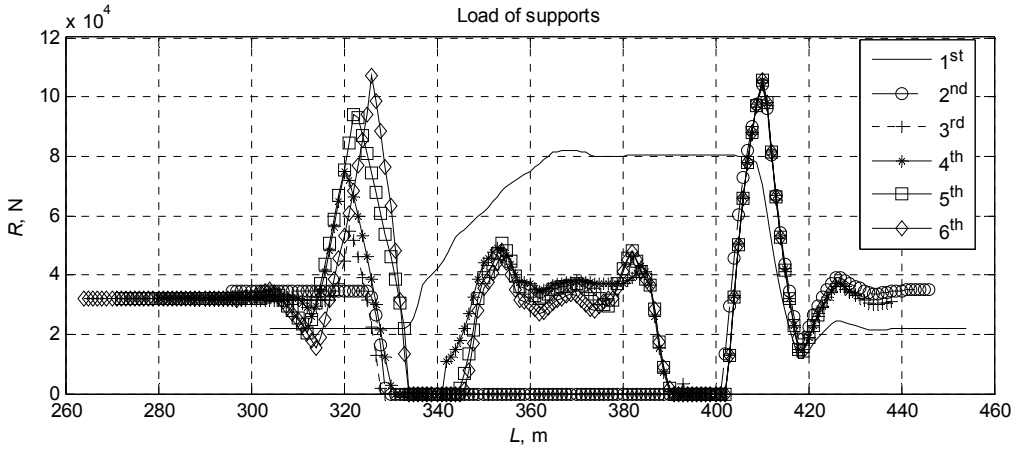

Fig. 13 Reactions of six leading supports during simulated insertion; the path of the micro-tunnel as designed

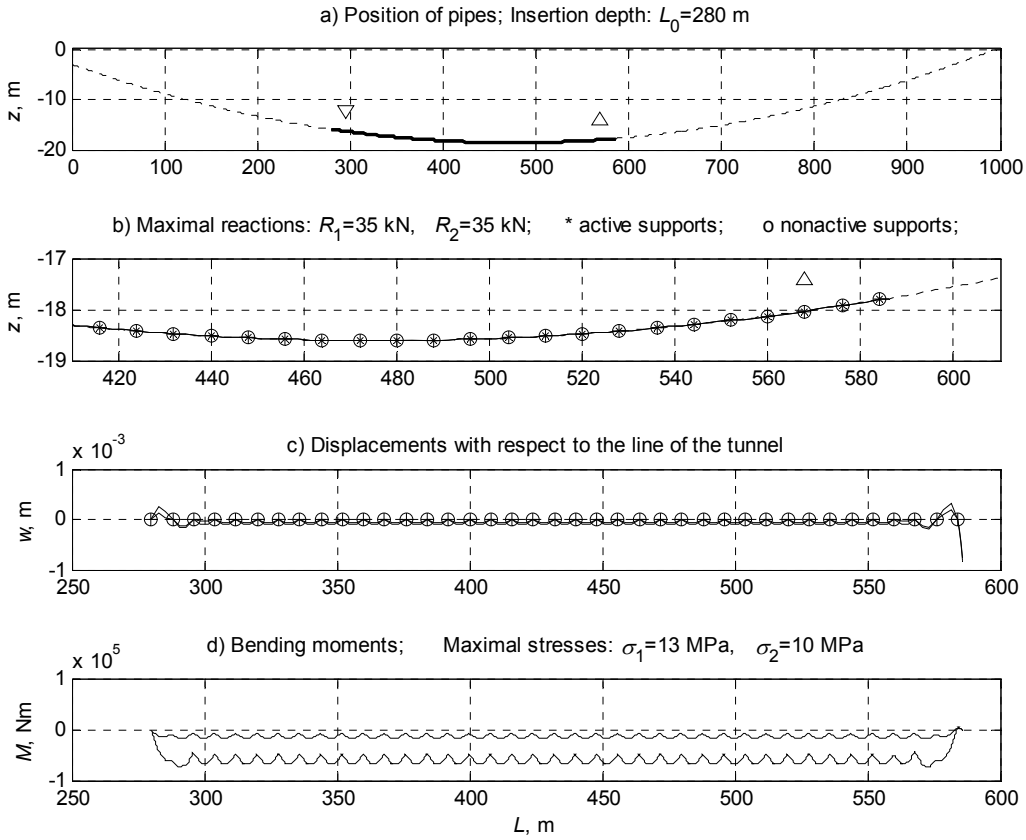

Fig. 14 Simulated insertion process at a given position of the pipe package segment in the micro-tunnel; the tunnel path is considered to be a perfect parabola

Thus, even a perfectly built path of the tunnel, if badly chosen, may lead to high values of support loads and bending moments, while a better selected, smooth curve can significantly reduce the load of the supports. This is shown in the simulation example of the ideal parabolic line path 3 (see Figs 14 and 15). With all supports in contact with the bottom of the tunnel, the reaction forces are reduced to 1/4 of the maximal initial value.

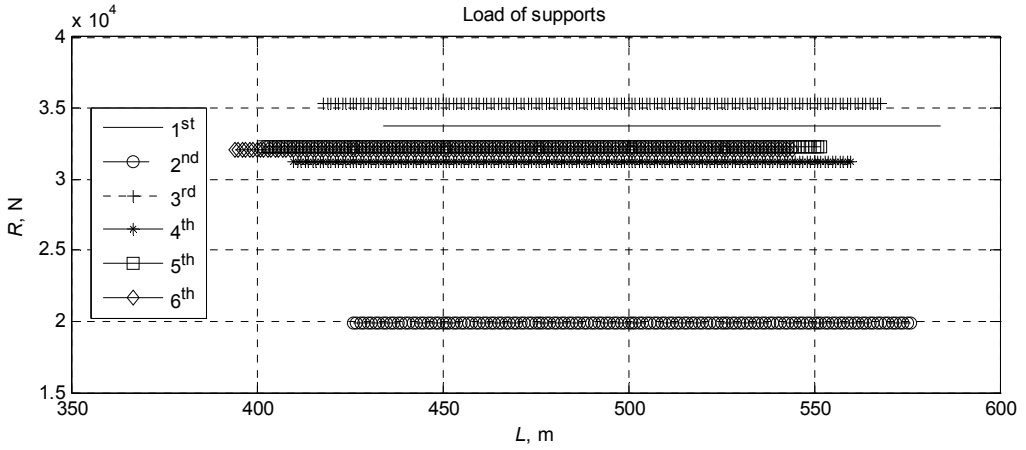

Fig. 15 Reactions of six leading supports during simulated insertion; the path of the micro-tunnel as a perfect parabola

By making the parabolic path more realistic, i.e. by increasing deviations of smooth, parabolic line to the values of the built path deviations of the studied case, maximal reactions

become equal to the original ones (see Figs 11 and 17), but the bending moments and stresses remain halved (see Figs 10d and 16d). Taking into account stress corrosion cracking [14,15], this will be an improvement if the pipeline is eventually immersed in the soil water.

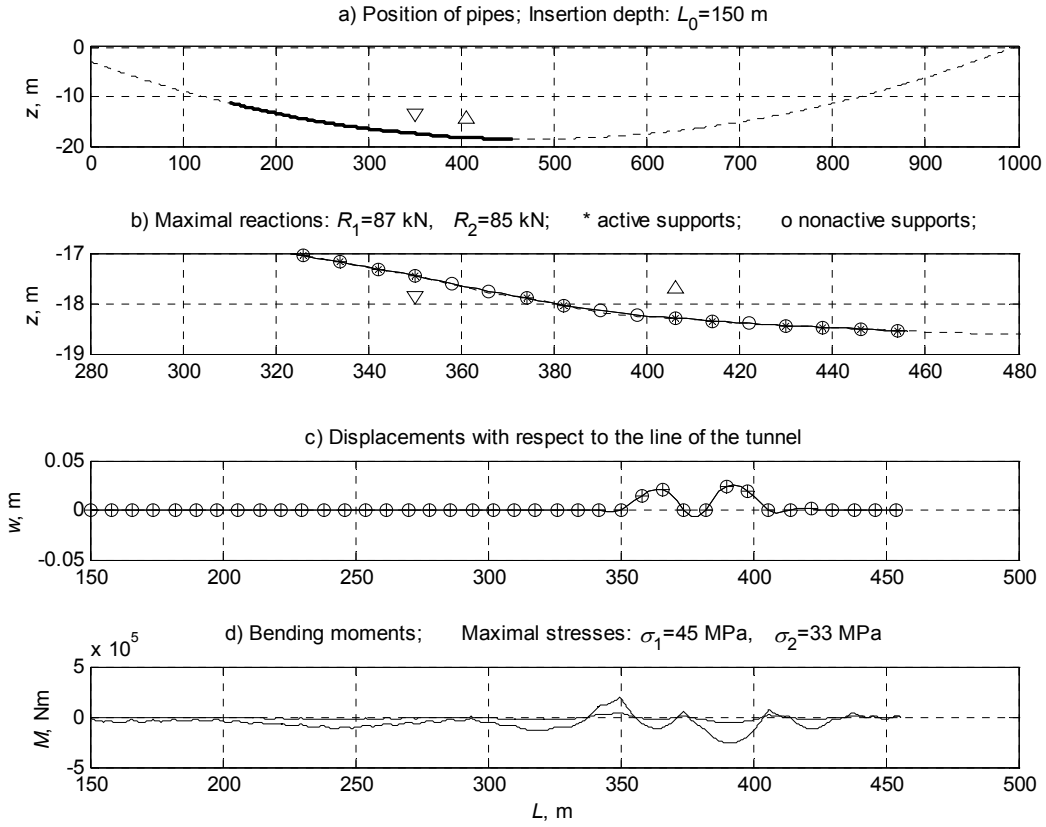

Fig. 16 Simulated insertion process at a given position of the pipe package segment in the micro-tunnel; the tunnel path is considered to be a distorted parabola

Technological advances in micro-tunnelling equipment [16,17] allow longer drives with greater accuracies. Recent accuracies reported in [18] are of ±20 mm in level and are finer than the standard tolerances [12]. Thus, performing the simulation with random deviations of that order, a smaller number of supports were lifted and maximal reactions were reduced to 40% of the initial value and the stress in pipes was further reduced (not shown in the figures).

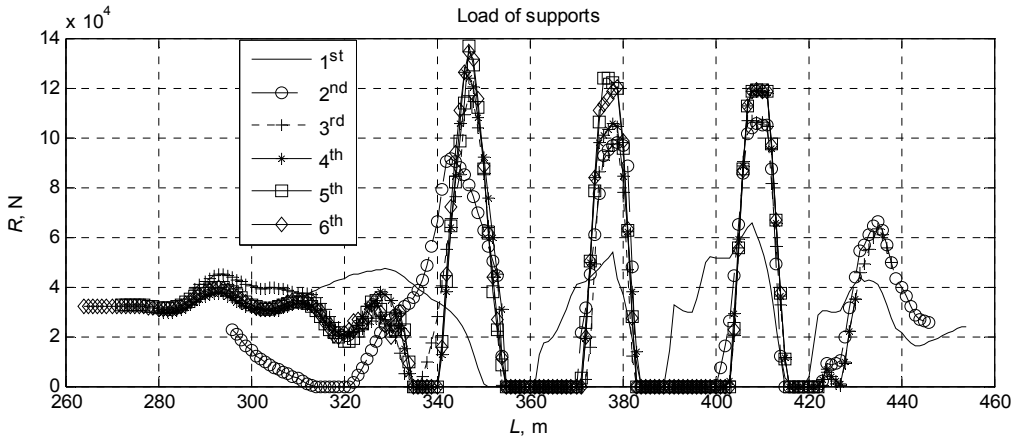

Fig. 17 Reactions of six leading supports during simulated insertion; the path of the micro-tunnel is a parabola distorted with deviations of the built path of the tunnel from the designed path

6. Conclusion

The insertion of a steel pipeline into an existing micro-tunnel presents a particular problem because the elastic line of the pipe under own weight does not, in general, coincide with the path line of the tunnel. Consequently, reactions are unevenly distributed among stiff wheel supports and the pipes are additionally stressed. A computational model is developed in order to determine the optimal distance between supports of steel pipes. Here, the following conditions are to be met: to satisfy the load limits on each support, to avoid contact with the ceiling of the tunnel, and to satisfy the strength requirements for both pipes. In the computational model, based on beam elements, the presented iteration procedure is applied for solving the unilateral contact problem.

Furthermore, this model is used for the investigation of the influence of a micro-tunnel path on the wheel support loading and pipeline stresses during the insertion and exploitation. The obtained results are useful for future micro-tunnelling practice. Four different paths of the micro-tunnel are studied for the same package of pipes on wheel supports: (i) path of the built tunnel, (ii) path as it was designed, (iii) ideal parabolic curve connecting the end points of the tunnel and of the same depth as the real tunnel, and (iv) parabolic curve distorted by the value of deviations of the built path from the designed one. It is shown that a carefully chosen path reduces the stresses in the pipes and, thus, makes the occurrence of corrosion stress cracking on the pipeline immersed in the soil water less probable.

Deviations of the micro-tunnel path from the designed line also have a strong influence on the load of the supports and the stresses in the pipes, but these deviations are greatly reduced by improvements in the current drilling technology, which has a significant influence on the reduction in both loads and stresses.

REFERENCES

[1] D. A. Willoughby, Horizontal Directional Drilling, Utility and pipeline applications, McGraw-Hill Companies, Inc. 2005.

[2] M. A. Polak, A, Lasheen, Mechanical modelling for pipes in horizontal directional drilling, Tunneling and Underground Space Technology, Vol. 16, Suppl. 1, S47-S55, 2002.

[3] E. Cheng, M. A. Polak, Theoretical model for calculating pulling loads for pipes in horizontal directional drilling, Tunneling and Underground Space Technology, Vol. 22, pp. 633-643, 2007.

[4] J. A. Cholewa, R. W. I. Brachman, I. D. Moore, Stress-strain measurements for HDPE pipe during and after simulated installation by horizontal directional drilling, Tunneling and Underground Space Technology, Vol. 25, pp. 773-781, 2010.

[5] J. Thomson, Pipe Jacking and Microtunneling, Blackie Academic & Professional, London, 1993.

[6] F. Giannessi, L. Jurina, G. Maier, A quadratic complementarity problem related to the optimal design of a pipeline freely resting on a rough sea bottom, Engineering Structures, Vol. 4, No. 2, pp. 75-85, 1982.

[7] F. Guarracino, V. Mallardo, A refined analytical analysis of submerged pipelines in seabed laying, Applied Ocean Research, Vol. 21, No. 6, pp.281-293, 1999.

[8] C. C. Baniotopoulos, F. Preftitsi, Influence of the design parameters on the stress state of saddle-supported pipelines: an artificial neural network approach, International Journal of Pressure Vessels and Piping Vol. 76, pp. 401-409, 1999.

[9] C. C. Baniotopoulos, Analysis of above-ground pipelines on unilateral supports: a neural network approach, International Journal of Pressure Vessels and Piping, Vol. 75, Issue 1, pp. 43-48, 1998.

[10] K. Thomopoulos, C. D. Bisbos, Unilateral contact stresses at steel pipe saddles, Thin-Walled Structures, Vol. 15 No. 4 pp. 305-319, 1993.

[11] M. L. James, G. M. Smith, J. C. Wolford, P. W. Whaley, Vibrations of Mechanical and Structural Systems, Harper & Row, Publishers, Inc. 1989.

[12] Pipe Jacking Association (PJA), Guide to the best practice for the installations of pipe jacks and microtunnels, London 1995.

[13] M. Vukšić, Insertion of pipes in a micro-tunnel, Degree thesis, FSB SZG, 2010.

[14] A. Contreras and S. L. Hernández and R. Orozco-Cruz and R. Galvan-Martínez, Mechanical and environmental effects on stress corrosion cracking of low carbon pipeline steel in a soil solution, Materials & Design, Vol. 35, pp. 281-289, 2012.

[15] F. M. Song, predicting the mechanisms and crack growth rates of pipelines undergoing stress corrosion cracking at high pH, Corrosion Science, Vol. 51, Issue 11, pp. 2657-2674, 2009.

[16] X. Shen, M. Lu, S. Fernando, S. M. AbouRizk, Tunnel boring machine positioning automation in tunnel construction, Gerontechnology Vol. 11(2):384, 1012.

[17] A. Jardon, S. Martinez, J. G. Victores, M. Marti, C. Balaguer, Extended range guidance system for micro-tunnelling machine, Gerontechnology, Vol. 11(2):326, 2012.

[18] X. S. Shen, M. Lu, W. Chen, Tunnel Boring Machine Positioning during Microtunneling Operations through Integrating Automated Data Collection with Real-Time Computing, Journal of Construction Engineering and Management, Vol. 137(1), pp. 72-85, 2011.

Submitted: 24.8.2012

Accepted: 22.02.2013

Doc. dr. sc. Nenad Kranjčević
Prof. dr. sc Milenko Stegić
Faculy of Mechanical Engineering and Naval Architecture
University of Zagreb

Mario Vukšić, mag. ing. mech.
Končar Generators and Motors inc.
Fallerovo šetalište 22, Zagreb